Water Level and Wave Height Estimates at NOAA Tide Stations from Acoustic and Microwave Sensors

JOSEPH PARK, ROBERT HEITSENRETHER, AND WILLIAM SWEET

National Oceanic and Atmospheric Administration, Silver Spring, Maryland

(Manuscript received 29 January 2014, in final form 9 May 2014)

ABSTRACT

The National Oceanic and Atmospheric Administration (NOAA) is transitioning the primary water level sensor at the majority of tide stations in the National Water Level Observation Network (NWLON) from an acoustic ranging system to a microwave radar system. Field comparison of the acoustic and microwave systems finds statistically equivalent performance when temperature gradients between the acoustic sensor and water surface are small and when significant wave height is less than roughly 0.5 m. When significant wave height is greater than approximately 0.5–1 m, the acoustic system consistently reports lower water levels. An analysis of 2 months of acoustic and microwave water level data at Duck, North Carolina, finds that the majority of differences between the two sensors can be attributed to systemic errors in the acoustic system and that the microwave system captures water level variability with higher fidelity than the acoustic system. NWLON real-time data products include the water level standard deviation, a statistic that can serve as a proxy for significant wave height. This study identifies 29 coastal water level stations that are candidates for monitoring wave height based on water level standard deviation, potentially adding a significant source of data for the sparsely sampled coastal wave fields around the United States, and finds that the microwave sensor is better suited than the acoustic system for wave height estimates.

1. Introduction

The National Oceanic and Atmospheric Administration (NOAA) National Ocean Service (NOS) manages the National Water Level Program (NWLP) to meet NOAA's mission requirements for coastal water level information. The NWLP is a major observational program within NOS and serves as a federal component of the Integrated Ocean Observing System (http://www.ioos.noaa.gov/) and the Global Sea Level Observing System (http://www.gloss-sealevel.org/). A fundamental component of the NWLP is the National Water Level Observation Network (NWLON), a network of more than 200 long-term, continuously operating water level stations around the United States, including island possessions, territories, and the Great Lakes (http://tidesandcurrents.noaa.gov/).

Since the early 1990s, the primary water level measurement system at most NWLON stations has been an acoustic time-of-flight range sensor encased in a protective well (Edwing 1991). From a logistical perspective, installation and maintenance of the protective well requires nontrivial infrastructure and yearly servicing including dive operations, and there is potential for the well to be damaged from flotsam or vessel impacts. The emergence of microwave water level sensors with substantially reduced installation and maintenance costs has motivated NOAA to transition from the acoustic systems to microwave sensors where possible (Heitsenrether 2009).

NOAA field evaluations comparing the two sensors find statistically equivalent performance at stations with little or no surface wave energy and small thermal gradients along the sounding tube. At stations with persistent surface waves larger than roughly 0.5–1-m significant wave height, monthly-mean water levels consistently reveal lower levels observed by the acoustic sensor. Boon et al. (2009) also reported differences between the acoustic and microwave system response with wave conditions, and Boon et al. (2012) presented evidence of an asymmetric water level distribution when

Denotes Open Access content.

Corresponding author address: Joseph Park, NOAA/NOS/CO-OPS, 1305 East–West Hwy., Silver Spring, MD 20910.
E-mail: joseph.park@noaa.gov

DOI: 10.1175/JTECH-D-14-00021.1

waves are present. To assess these differences, NOAA has been collecting acoustic and microwave water level data at NWLON stations located at the U.S. Army Corps of Engineers Field Research Facility (FRF) pier at Duck, North Carolina; Scripps Institution of Oceanography pier in La Jolla, California; and the William O. Lockhart Municipal Pier in Lake Worth, Florida. One of the primary goals of this paper is to assess comparative performance of the acoustic and microwave sensors in response to wave and temperature forcings for NOAA water level measurement and to attribute these differences to known physical responses of the sensor systems.

The other main goal is to characterize the relationship between significant wave height and NWLON water level standard deviations in order to facilitate use of the NWLON as a component of coastal wave observations. As surface wave amplitude increases, there is an increase in water level standard deviation (σ) for both the acoustic and microwave systems, although the relationship has been viewed primarily as a source of error in the water level measurement (Shih and Rogers 1981; Boon et al. 2012). However, as part of the Ocean Topography Experiment (TOPEX)/Poseidon validation experiments (Morris et al. 1995), Parke and Gill (1995) found a direct relationship between significant wave height ($H_{1/3}$) and standard deviation of the acoustic system. They concluded that standard deviation of the NOAA acoustic system is a good first-order measure of significant wave height; however, below a threshold wave height, the relationship degrades such that estimates of wave height are no longer viable. Given that the NWLON continuously monitors coastal water levels at numerous stations covering the U.S. coastline, a robust relationship between significant wave height and water level standard deviation could provide wave height estimates useful to coastal interests. Taking note of this, the Integrated Ocean Observing System (IOOS) plan for a surface wave monitoring network recognized that nondirectional wave data extracted from the NWLON can augment directional wave observations will be particularly useful for understanding the transformation and dissipation of waves as they traverse shallow and complex local bathymetry (IOOS 2009).

2. Sensors

a. Acoustic water level

The acoustic ranging sensor is coupled to a sounding tube that guides an acoustic pulse to the water surface; a complete description of the system can be found in Edwing (1991). The system is self-calibrating in the sense that it monitors the effective sound speed between the transducer and an acoustic reflector at a known distance (1.219 m), thereby adjusting for temperature-induced changes in sound speed. However, this assumes that the temperature near the transducer is representative of the mean temperature along the entire tube, and a potential error source arises from the strong temperature dependence of acoustic celerity if this assumption is violated (Porter and Shih 1996; Hunter 2003). When the sounding tube is longer than a few meters and the temperature difference between the upper section of the tube and the water surface is greater than a few degrees, water level errors of several centimeters are possible. Two temperature sensors (thermistors) are attached to the sounding tube to monitor temperatures along the tube with the upper sensor close to the acoustic transducer and the second sensor located above the highest astronomical tide. These temperature data are not used in the water level estimate, but they are collected so that temperature corrections can be applied in postprocessing (discussed in section 5).

The sounding tube is enclosed in a vented protective well, a 15.24-cm-diameter pipe extending below the water surface terminated with a brass orifice to restrict water mass transport in/out of the well. The depth of the water inlet is referred to as the submergence depth Y. When waves or other water level perturbations pass around the air–water interface, the response of the water level inside the pipe is delayed from frictional and inertial forces depending on the diameter of the well, the submergence depth, and the period and amplitude of the perturbations. The mismatch between the instantaneous water level inside and outside the well results in a buoyancy-driven oscillation of water level inside the well. Ignoring frictional effects and dependence of the protective well diameter, the natural period of oscillation is $T_n = 2\pi(Y/g)^{1/2}$, where g is the gravitational acceleration. For typical submergence depths of 4–6 m at coastal locations, T_n ranges from 4 to 5 s. The water inlet orifice is sized to work with the protective well to impose a mechanical low-pass filter on these pressure-induced water level variations and has a cutoff period of approximately 5 s.

Significant effort was expended in the 1980s with a series of laboratory, field, and numerical experiments to design the protective well based on hydrodynamics and water level frequency response (Shih 1981; Shih and Rogers 1981). Figure 1 reproduces from Shih (1981) the dynamic water level response R inside the well to surface wave excitation of height H and period T with a damping factor $\zeta = d_w/d_o$, where d_w and d_o are the diameters of the protective well and orifice, respectively.

Examination of Fig. 1 reveals why the orifice has a diameter of $d_o = 5.08$ cm. With a protective well diameter

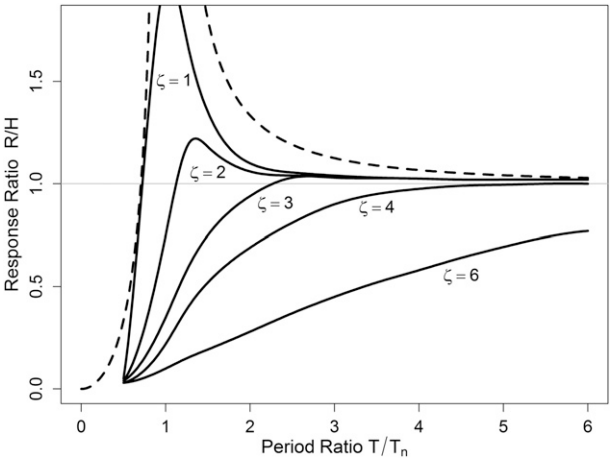

FIG. 1. Dynamic water level response R inside a protective well to surface waves of height H and period T from Shih (1981). Here T_n is the resonant period of the well and $\zeta = d_w/d_o$ is the damping factor where d_w and d_o are the diameters of the protective well and orifice, respectively. The dashed line represents the theoretical response in the absence of damping.

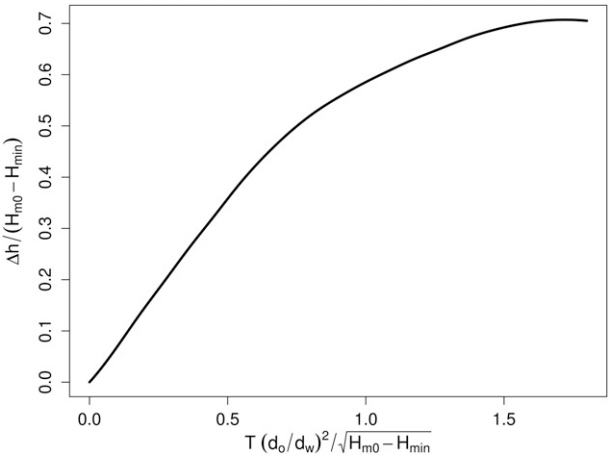

FIG. 2. Relationship between water level drawdown in centimeters (Δh) and surface wave forcing from Shih and Rogers (1981) Here T is the wave period, d_o/d_w the ratio of orifice to protective well diameter, H_{m0} the significant wave height in meters, and $H_{\min}$ minimum threshold wave height below which wave effects are not important.

of $d_w = 15.24$ cm, the value of ζ is 3, corresponding to a critically damped response. It is important to realize that Fig. 1 represents the response to a specific set of parameters: $H = 0.3$ m, orifice submergence depth $Y = 3.0$ m, and water depth = 7.6 m. Changing these parameters alters the shape and amplitude of the response curves, and it can be expected that the single-system design represented in Fig. 1 can behave quite differently under varying parameter regimes. For example, increasing the orifice submergence depth increases the amplitude response near resonance ($T = T_n$).

In addition to the resonant oscillations, Bernoulli's principle dictates conservation of pressure and velocity at the inlet orifice. When tidal- or wave-driven currents are significant across the orifice, the pressure reduction is known to draw down the water level inside the well. Shih and Rogers (1981) quantified the water level reduction as a function of wave height and period as shown in Fig. 2. We will use this function to assess water level differences between the microwave and acoustic systems in response to wave forcing. Again, it should be noted that while this curve applies to general combinations of wave height and period, protective well and orifice diameter, it is specific to an orifice hydraulic discharge coefficient of $C_d = 0.8$, an orifice submergence depth of 3 m, and a water depth of 9.14 m, and therefore it is expected to change under different regimes of water depth and orifice submergence depth.

b. *Microwave water level*

The microwave sensor operates at a frequency of 26 GHz with a beamwidth of 8°–10°, depending on the antenna. There is no contact with the water surface so that hydraulic effects from pressure variations do not influence the measurement. The sensor is remarkably insensitive to temperature variation (0.2 mm K^{-1}, 5-mm maximum) and has accuracy of ±0.03% of the measured range. However, microwave sensors have limitations, such as signal scattering/blockage from rain, ice or flotsam, sidelobe interference from pilings or other infrastructure, and a variable surface-area footprint dependent on sensor beamwidth and range from the water that introduces a spatial filter.

Details of the sensor can be found in Heitsenrether and Davis (2011). It is also notable that Boon et al. (2012) estimated the sensor accuracy of water levels and found a quadratic increase of sensor error with wave height.

c. *Wave height and period*

Hourly significant wave height (H_{m0}) and period were obtained from a Nortek bottom-mounted acoustic waves and current (AWAC) sensor operating at 1 MHz deployed on the same depth contour as the acoustic and microwave sensors (6 m) but located approximately 500 m northward.

3. Data

We present data and analysis from the NWLON station located on the U.S. Army Corps of Engineers FRF pier at Duck, a coastal location exposed to North Atlantic wave fields. Details of the NWLON station are available online at NOAA (2013b), a map and description of the test equipment and configuration are given in Boon et al. (2012), and details of the pier and

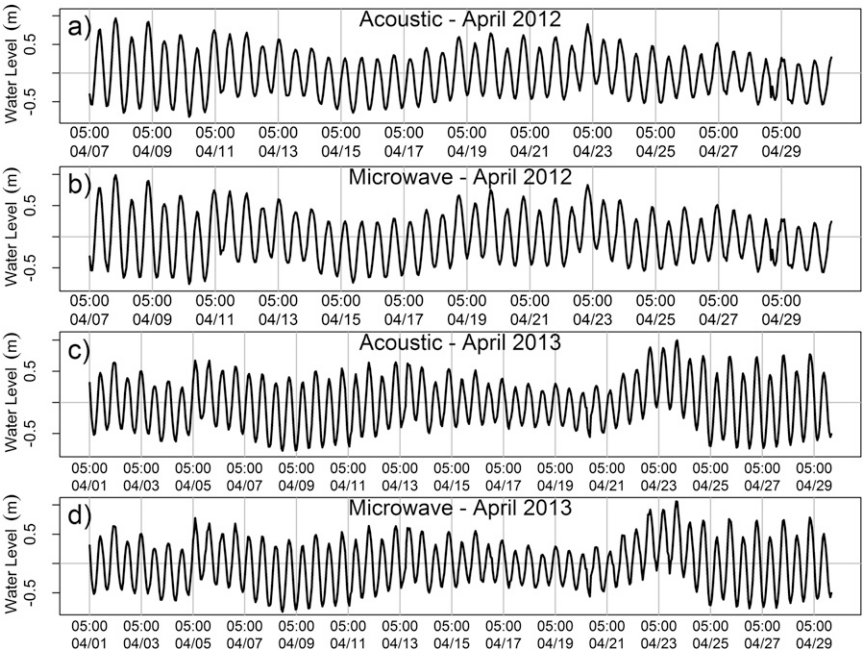

FIG. 3. Hourly water level estimates (UTC) from the acoustic and microwave sensors at Duck with the mean removed. (a) Acoustic sensor April 2012. (b) Microwave sensor April 2012. (c) Acoustic sensor April 2013. (d) Microwave sensor April 2013.

research facility are available online (http://www.frf.usace.army.mil/frf.shtml). Two datasets are examined in the analysis, the first covers 7–30 April 2012 and the second covers 1–29 April 2013. Data from La Jolla and Lake Worth (September–November 2013) have also been analyzed, finding results consistent with and corroborating the data and analysis presented here.

Raw range-to-water data were sampled from both the microwave and acoustic sensors at 1 Hz. These raw 1-Hz data were used in power spectral density (PSD) estimates (Fig. 6) and to compute the NOAA water level and standard deviation every 6 min. Mean range-to-water estimates are computed from raw 1-Hz range data by application of the NOAA data quality and assurance procedure (DQAP) (NOAA 2013a). This algorithm samples 181 consecutive 1-Hz values centered on each hour in 6-min intervals (minutes 0, 6, 12, 18, 24, 30, 36, 42, 48, 54) to compute an initial mean and standard deviation. Data points greater than three standard deviations from the mean are discarded, and a final mean and standard deviation are computed from the remaining points. These range data are transmitted by satellite to NOAA's Center for Operational Oceanographic Products and Services (CO-OPS), where they are converted to water level by subtracting the range estimates from the reference datum, which are then disseminated in near–real time on the Internet and stored in the NWLON archives. Our analysis uses hourly values consisting of one DQAP water level on the hour as shown in Fig. 3, where the mean has been removed. These hourly data are the basis for all analysis and statistics in this paper with the exception of the PSD estimates.

Figures 4 and 5 plot the difference between the hourly acoustic and microwave water levels, the temperature difference between the two thermistors, and significant wave height for April 2012 and April 2013, respectively. The water level differences are acoustic minus microwave, so that a positive differential implies the acoustic system reported a higher water level, a negative one that the acoustic level is lower. The temperature differences are upper thermistor minus lower thermistor, such that a negative differential represents a higher temperature along the sounding tube than at the acoustic transducer.

Two inferences are apparent from examination of Figs. 4 and 5. Positive water level differences appear related to negative temperature differentials along the sounding tube, and more clearly, negative water level differences are related to significant wave height. We examine each of these observations in the following sections, but first establish some general characteristics of the sensors with spectral analysis.

4. Acoustic and microwave frequency response

Examination of water level PSD estimates under different wave conditions reveals some fundamental

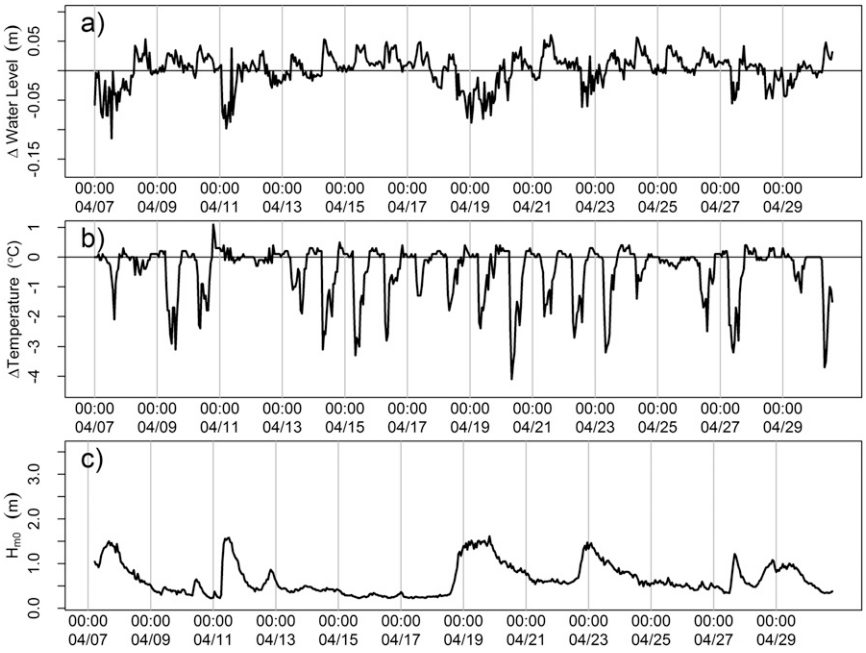

FIG. 4. Hourly data (UTC) from Duck in April 2012. (a) Water level difference between the acoustic and microwave sensors. (b) Temperature difference between the upper and lower thermistors of the acoustic sounding tube. (c) Significant wave height.

characteristics of the two systems. We estimate PSDs on the raw 1-Hz water level with a periodogram smoothed by a modified Daneill smoother of span 600 points, resulting in a spectral amplitude 99% confidence interval of 1.1 dB. Resultant PSDs for four distinct wave regimes are shown in Fig. 6. Figures 6a–c show spectra from waves of increasing height, all with dominant wave periods in the 7–15-s range. Figure 6d plots the response

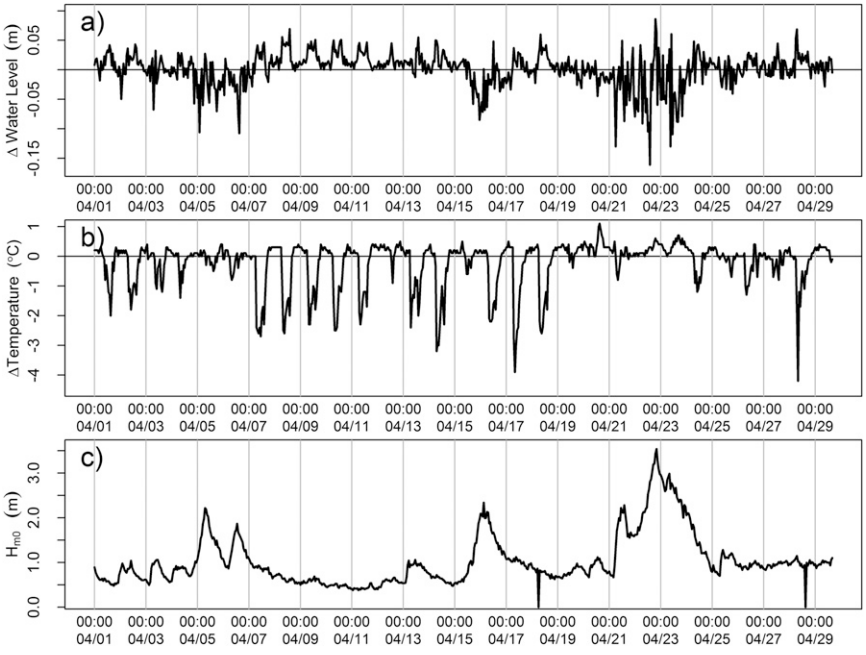

FIG. 5. Hourly data (UTC) from Duck in April 2013. (a) Water level difference between the acoustic and microwave sensors. (b) Temperature difference between the upper and lower thermistors of the acoustic sounding tube. (c) Significant wave height.

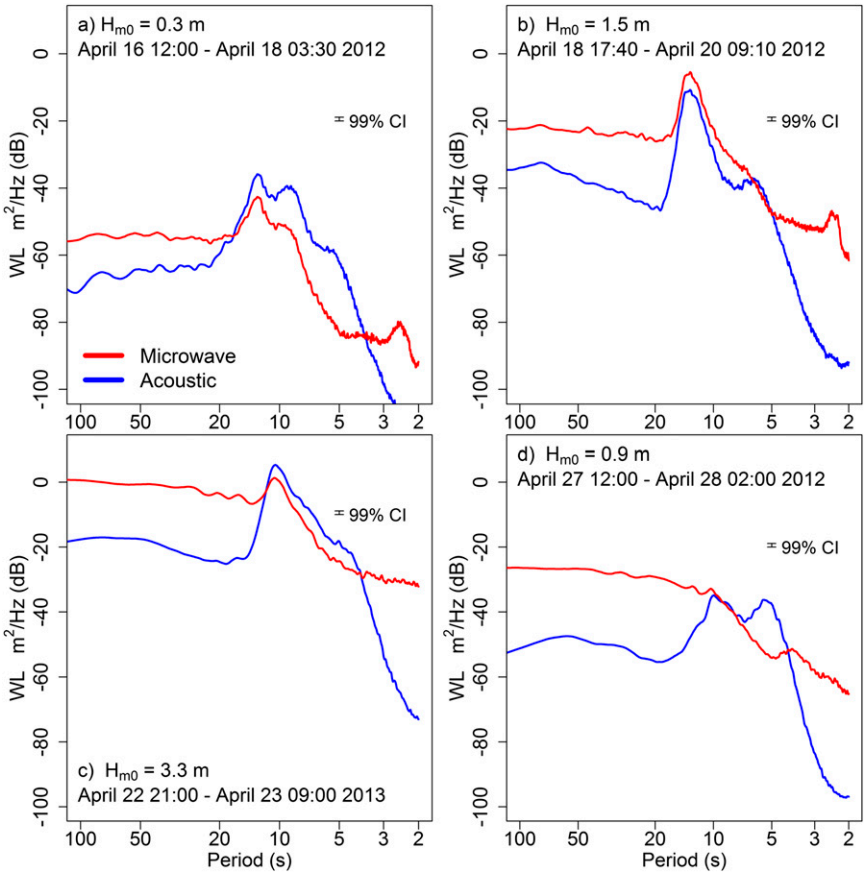

FIG. 6. Power spectral density estimates of 1-Hz water level data from the acoustic and microwave sensors. (a) Low wave conditions. (b) Intermediate to high wave conditions. (c) Very high wave conditions. (d) A locally generated short-duration wind-wave event with a dominant period of 4.1 s.

to a short-period (4.1 s) wave field generated by the passage of a cold front on 27 April 2012 (discussed in section 7).

Perhaps the most obvious characteristic is high-frequency attenuation of the acoustic system at periods shorter than about 5 s, owing to mechanical filtering from the water inlet orifice. Another robust feature observed across multiple datasets and environmental conditions is the enhanced response of the microwave sensor to water level variance from low to intermediate/high wave conditions in the wind-wave frequency band (periods of 5–20 s). This can be seen by comparison of Figs. 6a and 6b. In Fig. 6a the wave height is low and the microwave sensor water level variance is 5–10 dB less than that of the acoustic system. In Fig. 6b the wave height has increased by a factor of 5, and we find the microwave water level response is roughly 5 dB greater than that of the acoustic system. This ''inversion'' of water level variance translates into a superior water level sensitivity for the microwave sensor in the low to intermediate/high wave regime, and it led to identification of the microwave sensor as a higher fidelity water level sensor in the presence of waves (discussed in section 7).

Although the sensitivity of the microwave sensor to water level dynamics is greater than the acoustic system for low to intermediate/high wave conditions, we see in Fig. 6c that when waves are very high, the acoustic sensor reports higher variance in the 4–12-s band. NOAA is continuing to collect and analyze data in the high wave regime to ascertain whether it is a consistent characteristic between the two sensors.

Resonance of the protective well is a notable feature in Fig. 6d, where we see that the 4.1-s dominant wave period is captured by the microwave sensor, while the acoustic system responds with a broad peak around a period of 5 s. Evidence of the resonance is also seen in Fig. 6a, where the acoustic spectra has a ''knee'' at a period of 5 s, while the microwave presents no such energy. Examination of spectral coherence between the

acoustic and microwave sensors consistently finds values of coherence squared in the range of 0.7–0.8 over the wind-wave band, with values near zero at periods of 5 s and shorter. This lack of coherence when the resonance amplitude is significant indicates that the resonance is introducing a distortion to the water level power spectrum—that is, the water level variance associated with the resonance is not representative of the true water level dynamics outside the well, but of undamped oscillations inside the well. These resonance features are consistent with the dynamic response of the protective well being forced by combinations of parameters (wave height and period, orifice submergence depth, water depth, orifice discharge coefficient, etc.) that deviate from the ideal design represented in Fig. 1, such that the critically damped response is not realized.

At periods longer than 20 s, the two sensors respond with similar spectral shapes, but the microwave sensor consistently measures higher water level variance than the acoustic system. At these long periods, we are no longer dealing with direct-wind-generated ocean surface waves, but we are sampling infragravity waves and other nonlinear processes associated with subharmonics of wind waves, internal waves, edge waves trapped on the shelf, or other forcings (Munk 1951). It is not presently known whether this response represents an error in the microwave sensor, a higher fidelity sampling of low-frequency variability by the microwave sensor, a limitation imposed by the acoustic system mechanical filter, or some other effect.

5. Acoustic temperature dependence

In previous work investigating the relationship between temperature and accuracy of the acoustic ranging system, Porter and Shih (1996) described the system, the presently used correction algorithm, and assessed impacts with a case study at the La Jolla tide station. Their data reveal water level errors on the order of 5 cm arising from temperature-induced sound speed errors. Hunter (2003) conducted a comprehensive analysis of the temperature dependence, again finding the dominant error arising from uncertainty in sound speed.

It is worth noting that the current NWLON temperature correction algorithm makes a significant assumption concerning representation of the physical environment. The correction is

$$\Delta S = h(0.0018\Delta T), \tag{1}$$

where ΔS is the water level correction, h is the range from the acoustic transducer to the water surface, and ΔT is the difference between the temperature measured near the transducer and the temperature measured closer to the water surface. The factor 0.0018 is a constant relating the sound speed in an adiabatic ideal gas to temperature in units of degrees Celsius.

This correction contains no dependence on the location of the temperature measurements. For a given range to the water, the correction from ΔT measured over a distance of 1 cm is the same as for ΔT over a distance of 10 m. The assumption is that a stepwise constant temperature difference, one temperature at the sensor and another constant temperature along the sounding tube, accurately represents the effective temperature profile along the sounding tube. This first-order assumption may be valid in certain cases; however, in cases where the actual temperature profile is not well represented by a spatially independent temperature difference, the correction from Eq. (1) is known to be poor (Vogt et al. 1986). NOAA is currently exploring the use of additional thermistors and a spatially dependent algorithm to improve sound speed corrections. We note that for the data analyzed here, the temperature differences are less than 4.2°C, with mean and maximum sound speed changes of 0.6 and 2.5 m s^{-1}, respectively, resulting in temperature corrections of up to 7.2 cm.

As previously noted from inspection of Figs. 4 and 5, a relation between positive water level differences of the acoustic and microwave sensors and negative temperature difference of the two thermistors is evident. Even though the temperature correction of Eq. (1) is based on a simplistic physical model, it is the currently accepted algorithm and we use it to compute temperature corrections for the data shown in Figs. 4 and 5. These corrections are then compared with the observed water level differences as shown in Figs. 7 and 8, respectively. The acoustic temperature corrections are largely coherent with the positive water level differences with pronounced disagreement primarily arising when significant wave height is greater than 0.5 m. These discrepancies may reflect increased thermal mixing within the protective well driven by wind stress and pneumatic pumping from water level variance, since the protective well is vented at the top to allow ambient pressure equalization. The extent to which these positive water level differences are captured by the correction of Eq. (1) can be examined by linear regression of the positive sea level differences with the negative temperature differences for data having a wave height below a certain threshold. For the April 2012 data (Figs. 4 and 7), a threshold of $H_{m0} < 0.5$ m finds $r^2 = 0.49$ ($c = 0.86$, $p < 1 \times 10^{-9}$), while the April 2013 data finds $r^2 = 0.59$ ($c = 0.82$, $p < 1 \times 10^{-9}$), where c is the regression coefficient and p is the p value.

Comparison of a simple temperature correction model with observational data suggests that temperature-induced

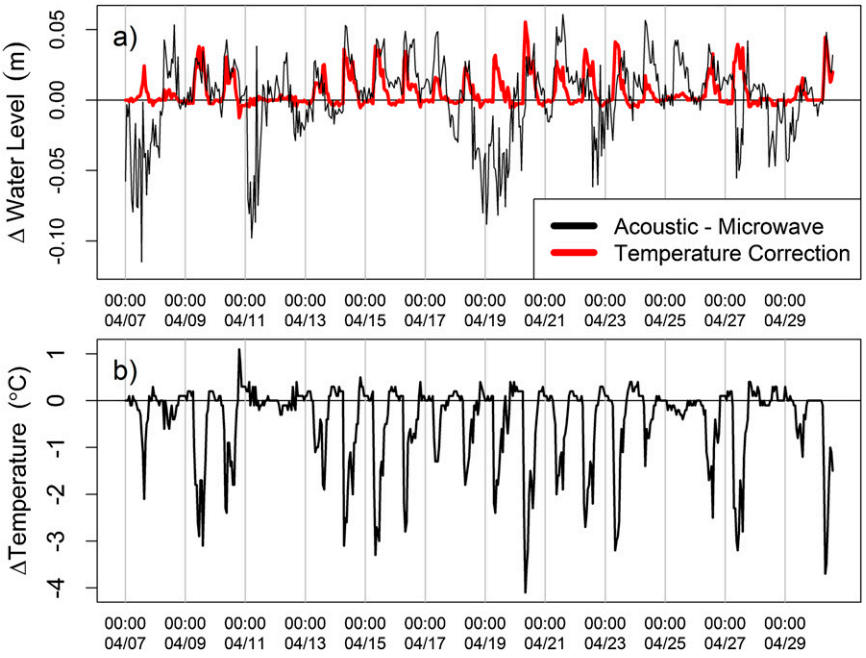

FIG. 7. Hourly data (UTC) and temperature corrections from Duck in April 2012. (a) Water level difference between the acoustic and microwave sensors (thin black line), and acoustic temperature water level change estimates (bold red line). (b) Temperature difference between the upper and lower thermistors of the acoustic sounding tube.

errors of acoustic water level are an important source of disagreement between the acoustic and microwave sensors.

6. Mechanical filter water level drawdown

To evaluate water level drawdown in the acoustic system, we apply the functional relation of Fig. 2 to both datasets (Figs. 4 and 5), with results presented in Figs. 9 and 10, respectively. One can see that the envelope of the drawdown model captures the overall negative water level differences; however, there are significant differences at short time scales (several hours), as positive water level differences are observed during wave events, for example, during the period 21–25 April 2013 (Fig. 10). It is not known whether these positive water level differences represent an error of the microwave sensor when water level variability is high (Boon et al. 2012), or whether it is a response of the acoustic system protective well and orifice. Water level pile up in the protective well is a known issue, and we suspect that these short time-scale differences are driven by resonance of water levels from a loss of damping.

To assess the drawdown model, we regress the envelope of negative water level differences against the predicted drawdown. The water level difference envelope is obtained from low-pass filtering the magnitude of the differences with an 18-h moving average filter and the result is $r^2 = 0.55$ ($c = 0.30$, $p < 1 \times 10^{-9}$) for the 2012 data, and $r^2 = 0.76$ ($c = 0.31$, $p < 1 \times 10^{-9}$) for the 2013 data. Not accounting for these wave-driven water level reductions in the acoustic sensors may impact long-term water level statistics. For example, based on the negative water level differences, the reduction in mean sea level between the acoustic and microwave water levels over the April 2012 and 2013 records are 1.1 and 1.0 cm, respectively.

We conclude that negative water level differences between the acoustic and microwave sensors are significantly driven by water level drawdown in the protective well due to wave-forced pressure fluctuations and currents.

7. Water level standard deviations and significant wave height

As wave energy increases, the standard deviation of water level estimates also increase. Parke and Gill (1995) evaluated this dependence for the acoustic system as part of the TOPEX/Poseidon validation at Platform Harvest, finding a linear increase of water level standard deviation with values in the range of 10–20 cm for significant wave height of 1 m. This is consistent with our data presented in Fig. 11 exploring the

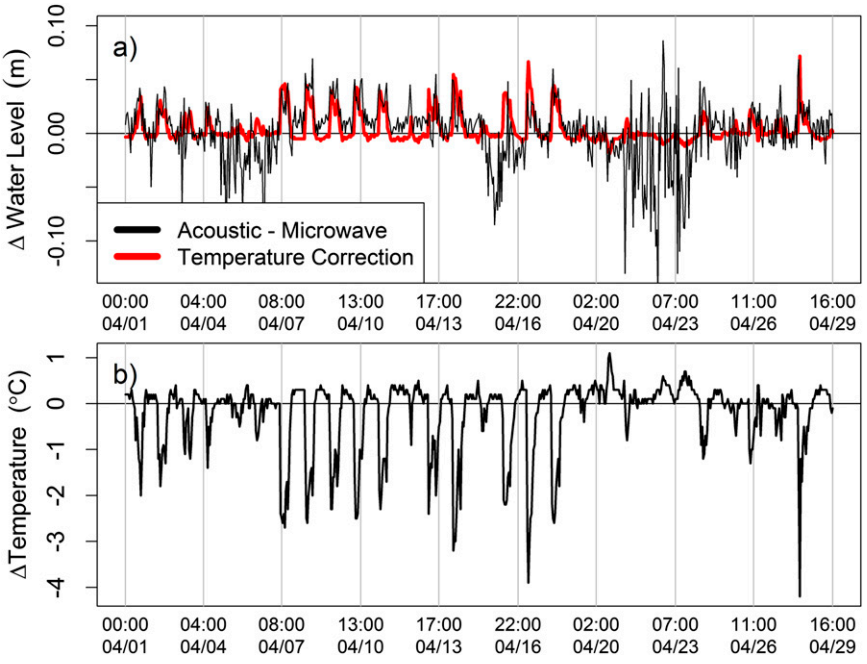

FIG. 8. Hourly data (UTC) and temperature corrections from Duck in April 2013. (a) Water level difference between the acoustic and microwave sensors (thin black line), and acoustic temperature water level change estimates (bold red line). (b) Temperature difference between the upper and lower thermistors of the acoustic sounding tube.

relationship between standard deviation and significant wave height at Duck, with standard deviation values in the range 7–20 cm for significant wave heights of 1 m.

A comparison of wave gauge hourly H_{m0} with water level standard deviations of the acoustic and microwave gauges over 24 days in April 2012 is shown in Fig. 11, suggesting a robust relationship between wave height and water level standard deviation. A direct estimation of H_{m0} from σ would utilize the canonical definition

$$H_{m0} = 4\sigma. \tag{2}$$

However, we recognize several factors can contribute to deviations from this ideal. One is that we are relating wave gauge H_{m0} estimated over a period of 1 h with a single σ estimated over 181 s. Other factors include the spatial separation (500 m) between the wave gauge and water level sensors, and water level measurement system mechanics. For example, the acoustic protective well introduces a nonlinear filter to the water level variance and this response is known to depend on wave height, period, and water depth (Shih and Rogers 1981); the microwave sensor images a variable footprint on the water surface depending on the sensor to water distance and implements some internal smoothing of the 1-Hz data. Therefore, we do not expect that NWLON water level σ will explicitly satisfy Eq. (2), but we can hope for a linear scaling and seek a parameter α that best relates water level σ to H_{m0}:

$$\hat{H}_{m0} = \alpha\sigma, \tag{3}$$

where $\hat{H}_{m0}$ is the estimate of H_{m0} and α is a factor that minimizes the residual $\epsilon = H_{m0} - \hat{H}_{m0}$. Fitting a linear model over the 24-day period results in $\alpha_\mu = 6.53$ and $\alpha_A = 11.08$ for the microwave and acoustic sensors, respectively, with the resulting $\hat{H}_{m0}$ shown in Fig. 12. The mean error of these first-order estimates can be represented with the RMS residual over the period and finds values of $\epsilon_\mu = 0.14$ m and $\epsilon_A = 0.21$ m for the microwave and acoustic sensors, respectively.

To assess the dynamics of this linear scaling on a finer temporal scale, we regress hourly H_{m0}/σ over a sliding window of length 24 h with the resultant fit and correlation coefficients shown in Fig. 13. Correlation and fit coefficients are only shown if the p value of the fit exceeds the 99% confidence level. The dashed line quantifies an ideal model of $H_{m0} = 4\sigma$, and we see that in a linear least squares sense the microwave sensor comes closer to this definition than the acoustic sensor. Both models find a significant dependence (p values < 0.01) during times of wave activity, and we note that in concordance with the expectation of Parke and Gill (1995) when wave activity is low (days 14, 17,

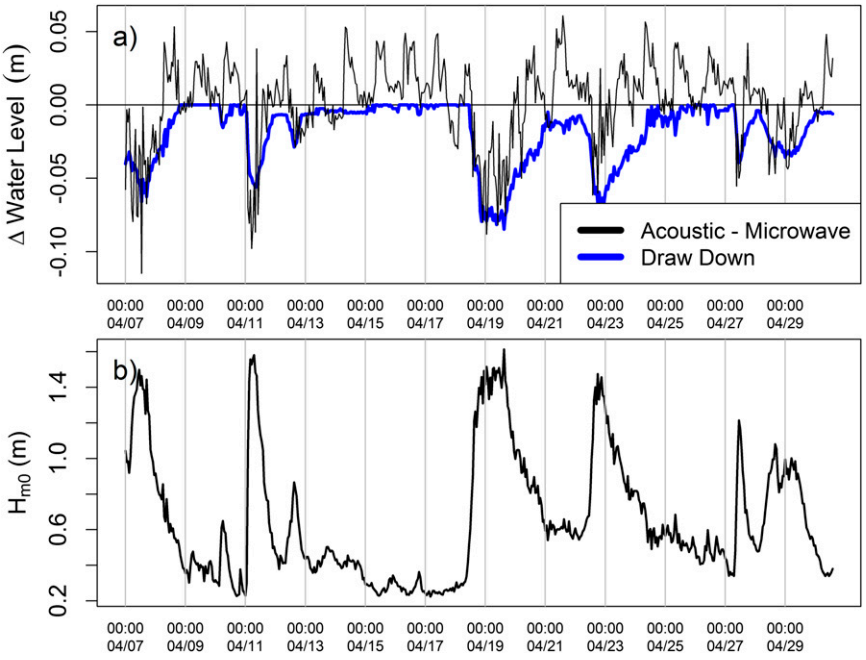

FIG. 9. Hourly data (UTC) and drawdown corrections from Duck in April 2012. (a) Water level difference between the acoustic and microwave sensors (thin black line), and protective well drawdown estimates. (b) Significant wave height.

24–27), the model fails to be statistically significant, although there are exceptions (days 9 and 30). Generally, the predictive skill of the acoustic system is less robust than that of the microwave system with consistently lower r^2 values and fit coefficients farther away from the ideal.

A reexamination of the acoustic and microwave water level σ shown in Fig. 11 reveals that the microwave

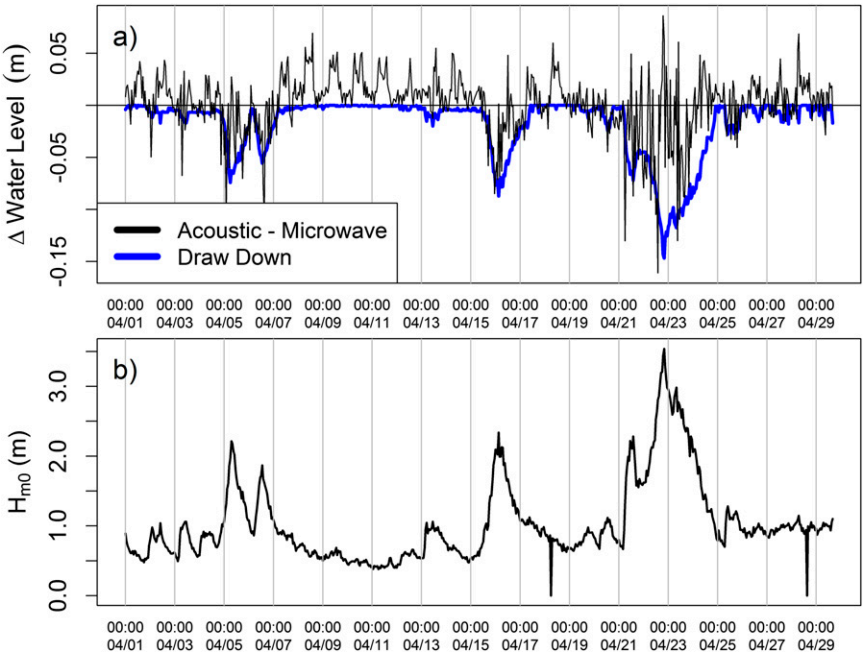

FIG. 10. Hourly data (UTC) and drawdown corrections from Duck in April 2013. (a) Water level difference between the acoustic and microwave sensors (thin black line) and protective well drawdown estimates. (b) Significant wave height.

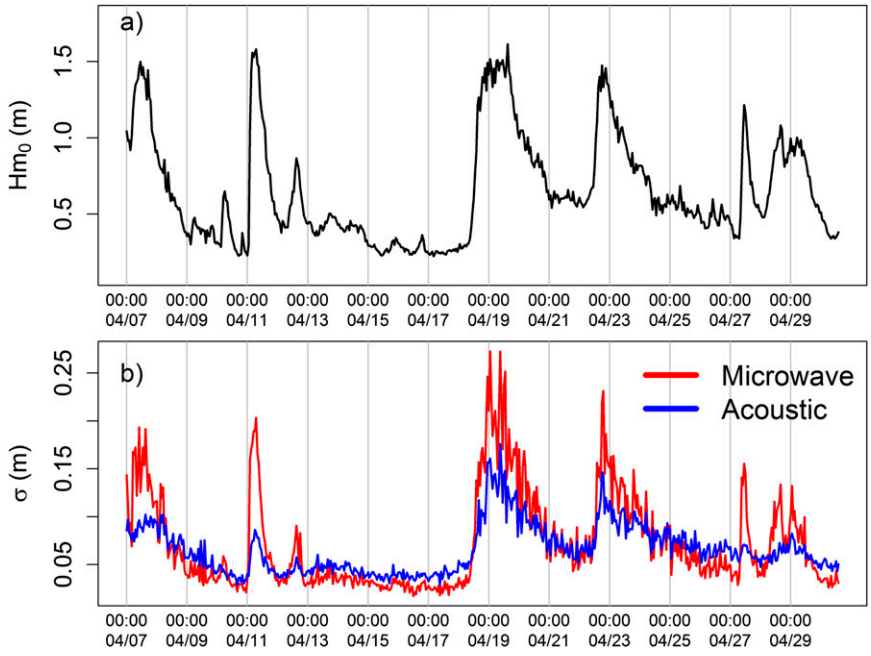

FIG. 11. (a) Hourly significant wave height H_{m0} during a 24-day period (UTC) in April 2012 at Duck. (b) Hourly NWLON standard deviations.

sensor exhibits a greater dynamic range than the acoustic system. During times of low σ, the microwave response is lower in amplitude than that of the acoustic system, whereas during times of high σ, the microwave response is higher. This suggests that in terms of water level variations, the microwave sensor has a higher sensitivity than the acoustic system, consistent with the spectral analysis presented in section 4.

Another difference evidenced in Fig. 11 during day 27 is that the microwave sensor exhibits a pronounced response to a short-term wave event, while the acoustic system presents only a minor indication (Fig. 11). Examination of meteorological data (NOAA 2012) reveals that a cold front moved through the area on 27 April with a change in wind direction from 270° to 10°–60° (offshore to onshore) with wind speeds during the period increasing from 5 to 10 m s^{-1} (10–20 kt; 1 kt = 0.51 m s^{-1}). These conditions are consistent with the formation of locally generated short-period wind waves. Wave gauge records over this period reveal an average wave direction of 64°, a height of 0.9 m, and a period of 4.1 s. Water level PSDs encompassing this event are shown in Fig. 6d, and we observe that at periods between 2 and 4 s, the acoustic system is attenuated from the low-pass mechanical filter by roughly 20 dB in relation to the microwave response, an amplitude ratio of 10 to 1. The microwave response reveals a small (3 dB) but statistically significant broad peak between 3 and 5 s, corresponding to the wave gauge report of a 4.1-s period. The combination of meteorological, wave gauge, and water level PSDs suggests that the wave event on 27 April was primarily locally generated short-period wind waves that the acoustic system filtered out, but which drove the protective well into a resonant water level oscillation at a period of 5 s.

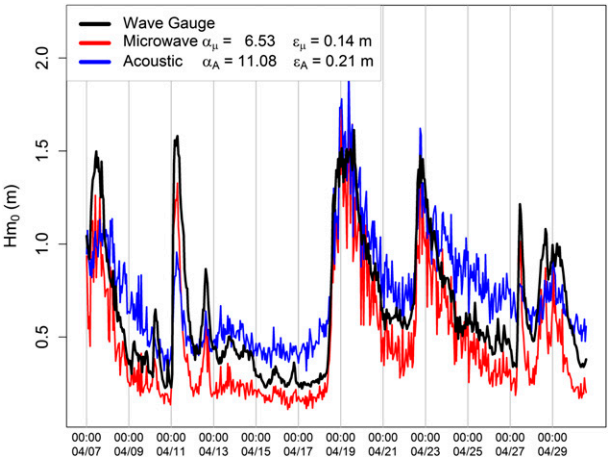

FIG. 12. Hourly significant wave height H_{m0} and estimates of wave height ($\hat{H}_{m0}$) from a linear model of H_{m0} regressed onto water level standard deviations (σ) over 24 days (UTC) in April 2012 at the Duck NWLON station. Term α is the least squares fit coefficient, ϵ is the RMS residual between wave gauge H_{m0}, and estimated wave height ($\hat{H}_{m0}$).

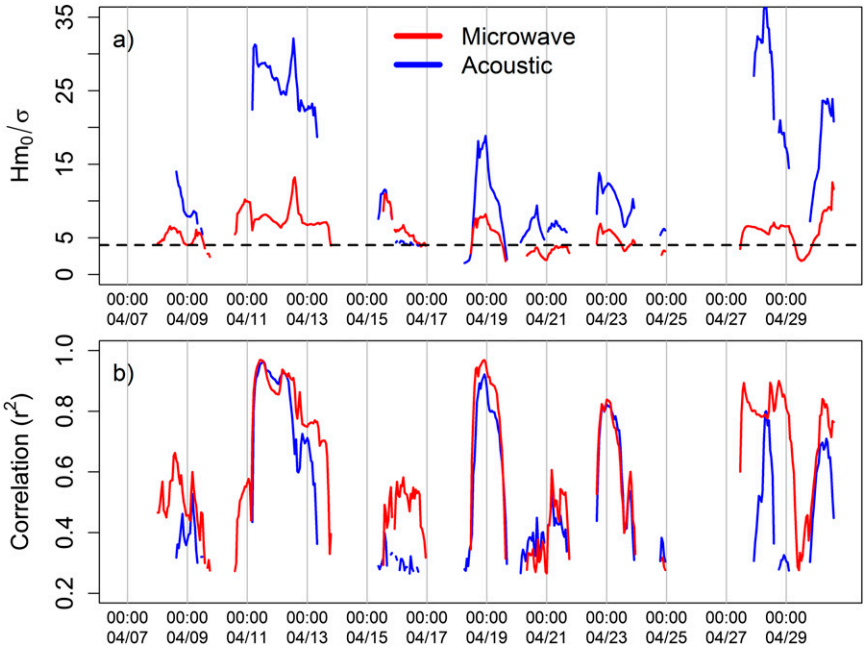

FIG. 13. Linear regression of the significant wave height (H_{m0}) onto the microwave and acoustic standard deviations shown in Fig. 11 over a 24-h sliding window (UTC). (a) Fit coefficients. The dashed line shows the ideal model of $H_{m0} = 4\sigma$, corresponding to the accepted definition of significant wave height. (b) Correlation coefficients. Values are shown only if the p value exceeded the 99% confidence level.

8. Prospective NWLON stations as wave proxies

As observed by Parke and Gill (1995) and evidenced in Fig. 13, there is a threshold of wave activity below which the linear model fails. Since many NWLON stations are in protected waters with limited wave activity, not all stations exhibit significant correlation with wave heights. Further study is needed to identify these thresholds. In the interim, NOAA has adopted an heuristic threshold to identify stations where wave activity is persistent. The metric is a 6-yr mean of monthly averaged water level standard deviation (σ) from the NWLON acoustic sensors, and persistent wave activity is associated with values greater than or equal to 2 cm.

There are 43 NWLON stations that exceed the 6-yr averaged threshold of $\sigma \geq 2$ cm, and ideally we seek to

TABLE 1. NWLON stations with 6-yr monthly averaged (January 2006–December 2011) water level σ that is equal or exceeds 2 cm and with significant correlations (p value < 0.01) between daily mean σ and ECMWF-Interim Re-Analysis daily H_{m0} greater than 0.3.

Station	r^2	6-yr σ (cm)	Station	r^2	6-yr σ (cm)
Duck, NC	0.43	14.0	Naples, FL	0.46	4.1
Wrightsville Beach, NC	0.42	11.9	San Francisco, CA	0.71	3.2
La Jolla, CA	0.57	11.5	Kahului, HI	0.34	3.0
Santa Monica, CA	0.32	11.0	Kawaihae, HI	0.32	2.9
Atlantic City, NJ	0.34	10.9	Bar Harbor, ME	0.46	2.5
Lake Worth Pier, FL	0.67	7.6	Chesapeake Bay Bridge Tunnel, VA	0.53	2.5
Port Orford, OR	0.53	7.0	Christiansted, St. Croix, VI	0.32	2.5
Arena Cove, CA	0.63	6.9	Kiptopeke, VA	0.35	2.4
Aguadilla Pier, PR	0.34	5.9	Seward, AK	0.46	2.4
Port San Luis, CA	0.54	5.1	Dauphin Island, AL	0.36	2.2
Westport, WA	0.80	5.1	Village Cove, Pribilof Island, AK	0.36	2.2
Monterey, CA	0.73	5.0	Crescent City, CA	0.64	2.1
Clearwater Beach, FL	0.44	4.9	Pago Pago	0.34	2.0
Point Reyes, CA	0.53	4.6	La Push, WA	0.68	2.0
North Spit, CA	0.72	4.2			

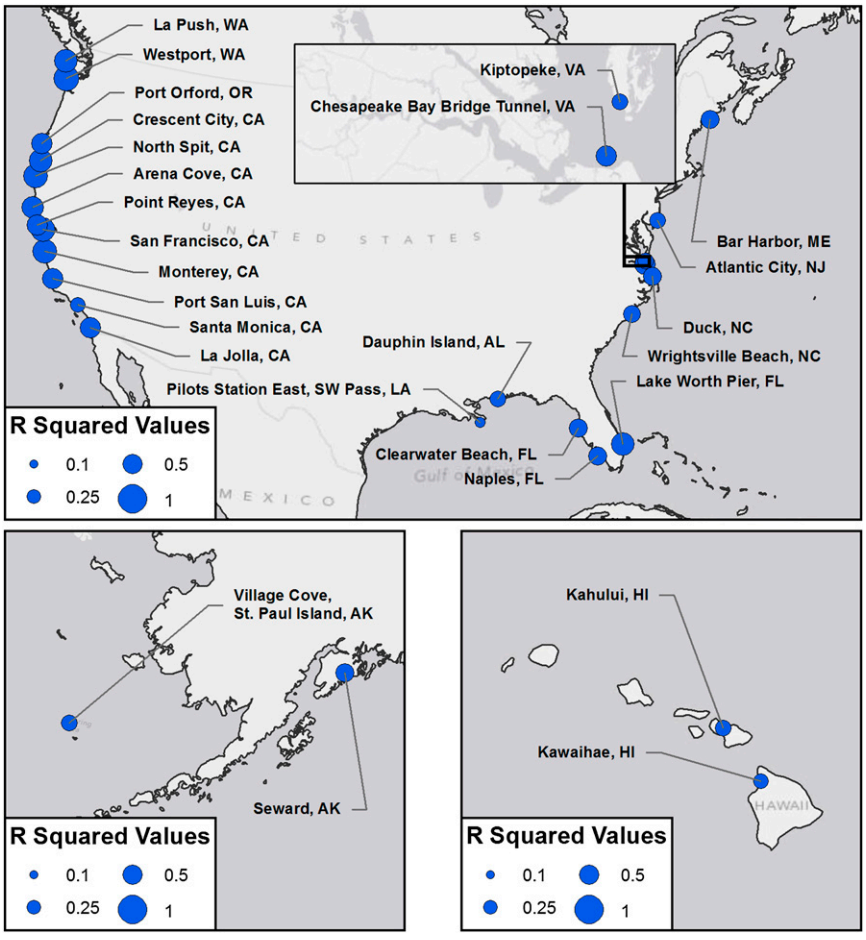

FIG. 14. Map of North American and Hawaiian NWLON stations from Table 1.

regress the σ of these stations against observational wave height data. Given the general lack of long-term observational wave data at these stations, we turn to the European Centre for Medium-Range Weather Forecasts (ECMWF) Interim Re-Analysis model. We regress daily mean water level σ to the ECMWF daily H_{m0} over the 6-yr period from 2006 through 2011. Given the coarse model domain (0.5° latitude and longitude), the daily time scale, and the neglect of nearshore wave transformation, we expect correlations will generally be low and use a threshold of $r^2 > 0.3$ at the 99% confidence level to select prospective stations. We find that 29 of the 43 stations meet this criterion and are listed in Table 1. A map of the North American and Hawaiian stations is shown in Fig. 14. We suggest that these 29 stations are good candidates for significant wave height estimates based on real-time water level σ.

9. Conclusions

As part of a modernization effort for NOAA's National Water Level Observation Network, acoustic ranging water level systems are being transitioned to microwave radar sensors. From a cost, maintenance, and support perspective, the microwave sensor is more efficient than the acoustic system, since it requires no infrastructure in contact with the water, although it has limitations to be considered. When used without a protective well, flotsam or surface ice can lead to erroneous water levels. We also find that ice accumulation in the antennas and scattering from heavy rain can degrade sensor performance. The use of a protective antenna cover (end cap) to prevent ice buildup inside the antenna does effectively mitigate the ice problem, but it introduces another problem, where moisture accumulation on the cover impedes the signal. The microwave beam pattern also needs to be evaluated to ensure that interference from pilings/mounting structures does not impede imaging of the water surface, and in surface wave sensing applications the footprint of the beam introduces a spatial filter (Heitsenrether et al. 2008).

Two benefits of the microwave sensor are that it is insensitive to temperature and it does not rely on

a hydraulic pressure measurement. With regard to temperature effects, our analysis finds that 49% and 59% of positive water level differences between the acoustic and microwave sensors at Duck during April 2012 and 2013, respectively, can be attributed to the speed of sound errors in the acoustic system. We expect that an improved temperature correction algorithm would find somewhat higher proportions. When a wave-induced water level drawdown model for the acoustic protective well is applied, we find that 55% and 76% of the negative water level differences during April 2012 and 2013, respectively, can be attributed to wave-induced pressure changes. Even though differences in water level response as a function of wave height are reasonably captured by the hydrodynamic drawdown in the protective well, there are notable exceptions during high wave events when a water level pile up is observed, and at infragravity frequencies the variance of the microwave system is higher than that of the acoustic sensor. Further study is needed to clarify these discrepancies. A third advantage of the microwave system is that there is no protective well and therefore no high-frequency water level resonances. We conclude that for the data analyzed here, the microwave sensor exhibits superior performance as a water level sensor when temperature gradients or waves are present.

NWLON data products recorded every 6 min include the standard deviation (σ) of 181 water levels sampled at 1 Hz. The σ statistic is known to be correlated with significant wave height, but it has been largely ignored as a wave height measure and viewed primarily as an error metric of water level estimates. To assess the link between water level standard deviation and significant wave height, a linear model significant at the 99% confidence level finds that the microwave sensor estimates significant wave height, and therefore water level variability, with higher fidelity than the acoustic system.

An assessment of NWLON stations for wave sensitivity was performed by identifying stations with 6-yr monthly-mean water level σ greater than or equal to 2 cm, and which correlated daily mean water level σ to the ECMWF-Interim Re-Analysis daily H_{m0} with r^2 greater than 0.3. This assessment selected 29 prospective stations as viable wave height proxies with the potential to provide a valuable addition to wave height estimation within the difficult and poorly sampled coastal zones. The relationship between wave height and water level σ should be calibrated at these stations through local field experiments. The availability of long-term coastal wave statistics at these stations can provide a significant contribution to the existing coastal wave observation network, and the length of the records opens the possibility of quantifying historical wave-proxy climatologies to examine storminess-related processes. Such weather-driven forcings are an important component of the total coastal water level, whose seasonal and interannual variability are poorly understood.

REFERENCES

Boon, J. D., R. M. Heitsenrether, and M. Bushnell, 2009: Microwave-acoustic water level sensor comparisons: Sensor response to change in oceanographic and meteorological parameters. *Proc. Oceans '09,* Biloxi, MS, IEEE/OES, 10 pp.

——, ——, and W. M. Hensley, 2012: Multi-sensor evaluation of microwave water level error. *Proc. Oceans'12,* Hampton Roads, VA, MTS/IEEE, 8 pp., doi:10.1109/OCEANS.2012.6405079.

Edwing, R. F., 1991: Next Generation Water Level Measurement System (NGWLMS): Site design, preparation, and installation manual. NOAA Tech. Rep., 213 pp. [Available online at http://tidesandcurrents.noaa.gov/publications/NextGenerationWaterLevelMeasurementSystemMANUAL.pdf.]

Heitsenrether, R. M., 2009: Using microwave range sensors for long term remote sensing of ocean surface dynamics. *17th Conf. on Atmospheric and Oceanic Fluid Dynamics,* Stowe, VT, Amer. Meteor. Soc., 8.2. [Available online at https://ams.confex.com/ams/17Fluid15Middle/webprogram/Paper154150.html.]

——, and E. Davis, 2011: Limited acceptance of the design analysis WaterLog H-3611i microwave radar water level sensor. Test and Evaluation Rep., NOAA Tech. Rep. NOS CO-OPS 061, 97 pp. [Available online at http://tidesandcurrents.noaa.gov/publications/Technical_Report_NOS_CO-OPS_061.pdf.]

——, M. Bushnell, and J. Boon, 2008: Understanding the impact of surface waves on microwave water level measurements. *Proc. Oceans '08,* Quebec City, QC, Canada, IEEE/OES, 8 pp., doi:10.1109/OCEANS.2008.5151923.

Hunter, J. R., 2003: On the temperature correction of the Aquatrak acoustic tide gauge. *J. Atmos. Oceanic Technol.,* **20,** 1230–1235, doi:10.1175/1520-0426(2003)020<1230:OTTCOT>2.0.CO;2.

IOOS, 2009: A national operational wave observation plan. Integrated Ocean Observing System Tech. Rep., 76 pp. [Available online at http://www.ioos.noaa.gov/library/wave_plan_final_03122009.pdf.]

Morris, C. S., S. J. DiNardo, and E. J. Christensen, 1995: Overview of the TOPEX/Poseidon Platform Harvest verification experiment. *Mar. Geod.,* **18,** 25–37, doi:10.1080/15210609509379740.

Munk, W. H., 1951: Origin and generation of waves. *Proceedings of First Conference on Coastal Engineering,* J. W. Johnson, Ed., Vol. 1, Council on Wave Research, 1–4.

NOAA, 2012: Meteorological observations, Duck, NC. Station ID: 8651370, NOAA. [Available online at http://tidesandcurrents.noaa.gov/data_menu.shtml?bdate=20120427&edate=20120428&metinterval=&unit=1&shift=g&stn=8651370+Duck%2C+NC&type=Meteorological+Observations&format=View+Plot.]

——, 2013a: Environmental measurement systems: Sensor specifications and measurement algorithms. NOAA CO-OPS, 9 pp. [Available online at http://tidesandcurrents.noaa.gov/publications/CO-OPS_Measure_Spec_07_July_2013.pdf.]

——, 2013b: Station information, Duck, NC. Station ID: 8651370, NOAA. [Available online at http://tidesandcurrents.noaa.gov/stationhome.html?id=8651370.]

Parke, M. E., and S. K. Gill, 1995: On the sea state dependence of sea level measurements at Platform Harvest. *Mar. Geod.,* **18,** 105–111, doi:10.1080/15210609509379746.

Porter, D. L., and H. H. Shih, 1996: Investigation of temperature effects on NOAA's Next Generation Water Level Measurement System. *J. Atmos. Oceanic Technol.,* **13,** 714–725, doi:10.1175/1520-0426(1996)013<0714:IOTEON>2.0.CO;2.

Shih, H. H., 1981: The water level response inside an open protective well to surface wave excitation. NOAA Tech. Rep., 47 pp.

——, and D. Rogers, 1981: Error analysis for tide measurement systems utilizing stilling wells. NOAA Tech. Rep., 113 pp.

Vogt, C. J., A. Croucher, and J. Mooney, 1986: The Aquatrak water level sensor field test at Shady Side, Maryland. STD-N-494, Submarine Technology Dept., Johns Hopkins University Applied Physics Laboratory, 66 pp.